THE JOURNAL OF PHYSICAL CHEMISTRY C

Article

pubs.acs.org/JPCC

Complex Oscillation Patterns During the Catalytic Hydrogenation of NO_2 over Platinum Nanosized Crystals

Cédric Barroo,[†,‡] Yannick De Decker,[‡,§] Thierry Visart de Bocarmé,[†,‡,*] and Norbert Kruse[†,‡,*]

[†]Chemical Physics of Materials - Catalysis and Tribology, Université Libre de Bruxelles (ULB), CP243, Brussels, Belgium

[‡]Interdisciplinary Center for Nonlinear Phenomena and Complex Systems (CENOLI), Université Libre de Bruxelles (ULB), Brussels, Belgium

[§]Non Linear Physical Chemistry Unit, Université Libre de Bruxelles (ULB), CP231, Brussels, Belgium

ABSTRACT: We studied the catalytic reduction of NO_2 with hydrogen on platinum model catalysts by means of field emission techniques. Atomic resolution field ion microscopy (FIM) was used to characterize Pt samples conditioned as tips. The catalytic reaction was investigated with video frequency resolution using field electron emission microscopy (FEM). Kinetic instabilities eventually merging into self-sustained periodic oscillations were observed. Data analyses revealed monomodal and bimodal oscillations as well as the coexistence of both mono- and bimodal regimes. Fourier transforms and interpeak intervals were used to characterize these different modes. We propose a mechanism that qualitatively explains the emergence of oscillations and the appearance of bimodal oscillations.

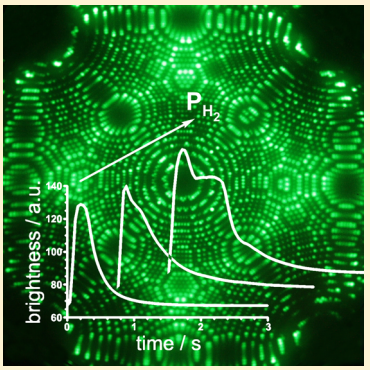

1. INTRODUCTION

Since their early development by E. W. Müller,[1,2] field electron emission microscopy (FEM) and field ion microscopy (FIM) have been widely used to image and characterize the structure of materials prepared as tips and to follow surface dynamics with nanoscale lateral resolution. Surface diffusion,[3,4] adsorption,[5−7] and surface segregation[8,9] are some of the fields that have been investigated this way. These methods also allow real time reaction kinetics to be observed, as well as morphological changes of the sample, under truly in situ conditions and with a nanometric or, ultimately, atomic resolution.[10−15]

Such studies are of pivotal importance for the understanding of the catalytic behavior of metallic particles. Indeed, because of their size and morphology, the apexes of the samples can be considered excellent models of single catalyst grains.[16−18] Metallic tips as used in FIM and FEM studies have a quasi-hemispherical apex presenting various facets of different orientations. Such facets do not behave independently in the course of a catalytic reaction. Adjacent crystal planes are coupled via surface diffusion of adsorbates which is known to influence the kinetics.[19] This is highlighted by the size and shape effects of nanoparticles on the catalytic activity: bigger nanoparticles exhibit extended facets as well as facets of higher indices than smaller nanoparticles. The synergy between those facets may enhance the catalytic activity.[20,21] In the case of surface reactions involving different chemical species, this complexity may lead to inhomogeneity in the adsorbate coverages and, eventually, to time-varying patterns, which translate into brightness signals on the screen of the microscope. The local surface processes can thus be investigated by monitoring the local brightness during the ongoing catalytic reaction.

In such experiments, the system is usually kept far from chemical equilibrium.[22] The metallic tip serves as a nanosized catalyst in steady flow conditions. These experimental conditions may lead to the emergence of complex phenomena, such as spatial and temporal symmetry breaking.[23,24] The breaking of space symmetry can appear in the form of chemical wave propagation or regular patterns, while the breaking of time symmetry typically reveals itself through the emergence of nonlinear dynamics such as aperiodic and periodic oscillations, chaos, and so on.[25] The emergence of such instabilities is often characterized by sudden qualitative changes of the dynamical properties of the system, for example, bifurcations, which are observed for a specific combination of the control parameters, such as temperature, partial pressures of the reactants, or electric field strengths. Successive bifurcations typically lead to an increasing level of complexity in a system. Many complex behaviors have been reported in the case of nonequilibrium reactions, including surface processes.[26−30] Simple periodic oscillations,[31] quasi-periodicity,[32] period doubling,[33] intermittency,[34] and mixed mode oscillations[35−37] have all been identified at mesoscopic and macroscopic scales.[38−40] From a more microscopic point of view, these phenomena can be seen as a collective response of reactive molecules to external constraints. Nonequilibrium statistical mechanics actually predicts collective responses, such as the aforementioned

Received: December 20, 2013
Revised: March 7, 2014
Published: March 11, 2014

   dx.doi.org/10.1021/jp412506e | J. Phys. Chem. C 2014, 118, 6839−6846

oscillations, which appear in systems with large amounts of molecules. Nanosized systems are expected to be characterized by strongly fluctuating dynamics. Indeed, it is known that the relative fluctuations scale as the inverse of the square root of the number of particles, as long as a system evolves far from any bifurcation point. Fluctuations may thus significantly influence the dynamics of nanoscale reactions, leading to essentially erratic collective behaviors (as compared to periodic oscillations at the macro- and mesoscale). Furthermore, the presence of inherent fluctuations may induce transitions that cannot be observed at larger scales.[41−43]

However, regular periodic phenomena also exist at the nanoscale. This feature is important not only for the kinetics of catalytic systems, but also for the dynamics of nanoreactors, globally speaking. This includes, for example, the very possibility of having regular oscillations in biological cells. Previous studies of the CO + O_2 reaction demonstrated the existence of oscillations at such small scales.[13,42,44] In this work, we report additional observations supporting this idea. Using FEM, we prove the existence of robust monomodal and bimodal periodic oscillations for the catalytic NO_2 + H_2 reaction over platinum nanocrystals. The technical details concerning both the experimental and theoretical techniques leading to such conclusions are given in section 2. In section 3 we show how the experimental results prove the existence, at the nanometric level, of regular oscillatory behavior that was previously only observed at much larger scales. Such collective behaviors thus seem to be very robust, even under the influence of spontaneous compositional fluctuations. The fourth section is devoted to a discussion on the physicochemical mechanisms behind the observed dynamics. We finish by discussing the potential consequences and possible extensions of our work.

2. METHODS

2.1. Experimental Setup. The experiments were carried out in a stainless steel field ion microscope with a base pressure of 10^{-8} Pa. Details about the setup and principles of the methods can be found elsewhere.[45] Platinum field emitter tips, used here as model catalysts, were electrochemically etched in a molten salt mixture of $NaCl/NaNO_3$ (1:4 w/w). The samples were then cleaned in a UHV chamber by cycles of treatment consisting of the following:

- Field evaporation of the tip in the presence of neon, to remove the impurities and to provide a quasi-hemispherical morphology, the so-called field evaporation end form (conditions of evaporation: P_{Ne} = 10^{-3} Pa, F_{tip} = ∼45 V/nm, T = 120 K).
- Annealing to increase the mobility of atoms and to reduce the risk of sample fracture due to the presence of stacking defects or grain boundaries (conditions: UHV, no applied electric field, T = 600 K during 15 min).
- Ion sputtering in the presence of neon, to decrease the radius of curvature of the apex (conditions: P_{Ne} = 10^{-3} Pa, F_{tip} = 6 V/nm, T = 400−600 K, tip is at inversed polarity as compared to FIM or field evaporation).

For the reaction experiments, field electron microscopy was used. The influence of the electric field on the local chemistry is less intense in this case as compared to field ionization conditions. Furthermore, the risk of fracture of the sample during FEM imaging is strongly reduced this way. Typical procedures consisted in heating the sample to 390 K and applying a field of 4 V/nm. A mixture of nitrogen dioxide (98% purity) and dihydrogen (99.9996% purity) was then admitted into the chamber, and once the reaction was triggered, the dynamic pattern formation was followed by a video camera with a time resolution of 40 ms and digitized with a dynamic range of 8 bits.[46] The dynamics of the process was analyzed by measuring the variations of gray levels with time, image by image. Due to the high amplitude of brightness variations, a linear response behavior of the detection system had to be ensured between the dark current and the signal saturation. The emitted electron current is amplified through a multichannel plate and then converted into photons. The recorded signal also comprises inherent noise and response to light of the recording device. Furthermore, an appropriate treatment of the brightness signal had to be provided. To do so, we applied the following procedure:

- Monitor the brightness over a region of interest (ROI) where surface reactions occur (no signal saturation occurring).
- For the same sequence, monitor the brightness over a region of the screen that does not comprise the image of the sample itself, that is, the dark current of the detector screen and recording device.
- Subtract the dark current from the monitored brightness in ROI and shift the resulting series by the flaw signal eventually captured due to parasitic coupling of the desired signal to the dark current (mainly during reaction events with large brightness change).

The ROI corresponds to the (012) facet and extends over approximately 10 nm^2.

2.2. Signal Treatment. The signal was analyzed using various time series analysis procedures. The periodicity of the time series was assessed through Fourier power spectra of the original signal, autocorrelation functions of the series and power spectra thereof. In order to illustrate the shape of the oscillatory profiles, we also performed periodic averages of the time series. To this end, the original data was divided into segments of length L, where L is the mean period of oscillation, in number of video frames. An average was performed over the measured signal brightness to obtain a single representative average oscillation. We built interpeak interval maps that plot the time interval between two successive peaks as a function of the previous such time interval.[47] These maps are used for the rationalization and classification of complex oscillatory phenomena.

3. EXPERIMENTS AND TIME SERIES ANALYSIS

This section reports on the reduction of NO_2 by H_2 on platinum at 390 K using FEM. A field ion micrograph of a typical as-prepared sample is shown in Figure 1a. The sample is imaged with atomic resolution and neatly divided into a number of high index planes located along the various zone lines between the central (001) pole and the peripheral planes. The Miller indices of some of the facets are indicated on the micrograph. For the sake of comparison, Figure 1b shows a top view of a (001)-oriented, hemispherically shaped ball model for a face-centered cubic system. The good agreement between the structure of the sample and that of the model is due to the fact that the FIM or FEM patterns result from the projection of ions or electrons, respectively, from the apex to the screen along the field lines. The crystallographic orientations of the facets appearing on the screen can thus be identified with respect to the ball model. This correspondence is crucial for determining

dx.doi.org/10.1021/jp412506e | J. Phys. Chem. C 2014, 118, 6839−6846

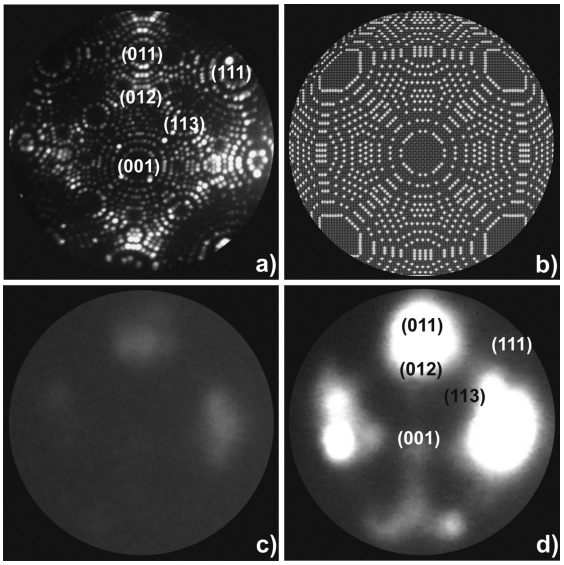

Figure 1. Imaging of the platinum nanocrystal before and during reaction: (a) Field ion microscopy micrograph of a platinum sample used as model catalyst - imaging conditions: $P_{Ne} = 1.0 \times 10^{-3}$ Pa, T = 55 K, $F_{tip} \approx 35$ V/nm. (b) Ball model of a hemisphere constructed according to an fcc crystal lattice (every single ball in the model corresponds to a single atom in the previous micrograph). (c) Field emission microscopy micrograph during reaction (imaging conditions: T = 390 K, $F_{tip} \approx 4$ V/nm), which exhibits a low brightness level due to the presence of adsorbed oxygen atoms on the surface. (d) Field emission microscopy micrograph during reaction. The higher brightness level is due to water formation and cleaning of the surface. The relatively low brightness of the symmetry-equivalent {011} region in the bottom part of the image is due to an asymmetry of the tip crystal (note the much larger {111} peripheral planes in the bottom part of (a) as compared to those in the top part).

where the local catalytic activity takes place when the sample is imaged with FEM, the spatial resolution of which is limited to ~2.5 nm under reactive conditions (Figure 1c,d).

In order to observe and classify the complex dynamical phenomena occurring during the NO_2 + H_2 reaction, the samples were subjected to a steady flow of reactants maintained by dynamic pumping. The tips were first heated to T = 390 K before introducing the gases. We typically started the experiments with bare NO_2, to which H_2 was added gradually until a mixture of desired P_{H_2}/P_{NO_2} pressure ratio was established. We detail below the different complex phenomena that were observed while varying the H_2 pressure, which acts here as the control parameter. We explain, in each case, how time series analyses were used in order to determine the class of nonlinear dynamical system they belong to.

3.1. Emergence of Oscillations. At low P_{H_2}/P_{NO_2} ratios, the image brightness remains low in the ROI (as defined in section 2), with values fluctuating within the range of the background noise. Intense transient brightness peaks could be observed intermittently when slowly increasing the hydrogen pressure. These bursts were found to merge into more regular patterns as the hydrogen pressure was further increased, eventually leading to very regular periodic oscillations. For example, Figure 2a depicts the time series of the brightness for a P_{H_2}/P_{NO_2} ratio of 7.2. Note that the oscillations present asymmetric peaks: after an abrupt rise, the brightness returned to its low value rather slowly. Remarkably, we could observe

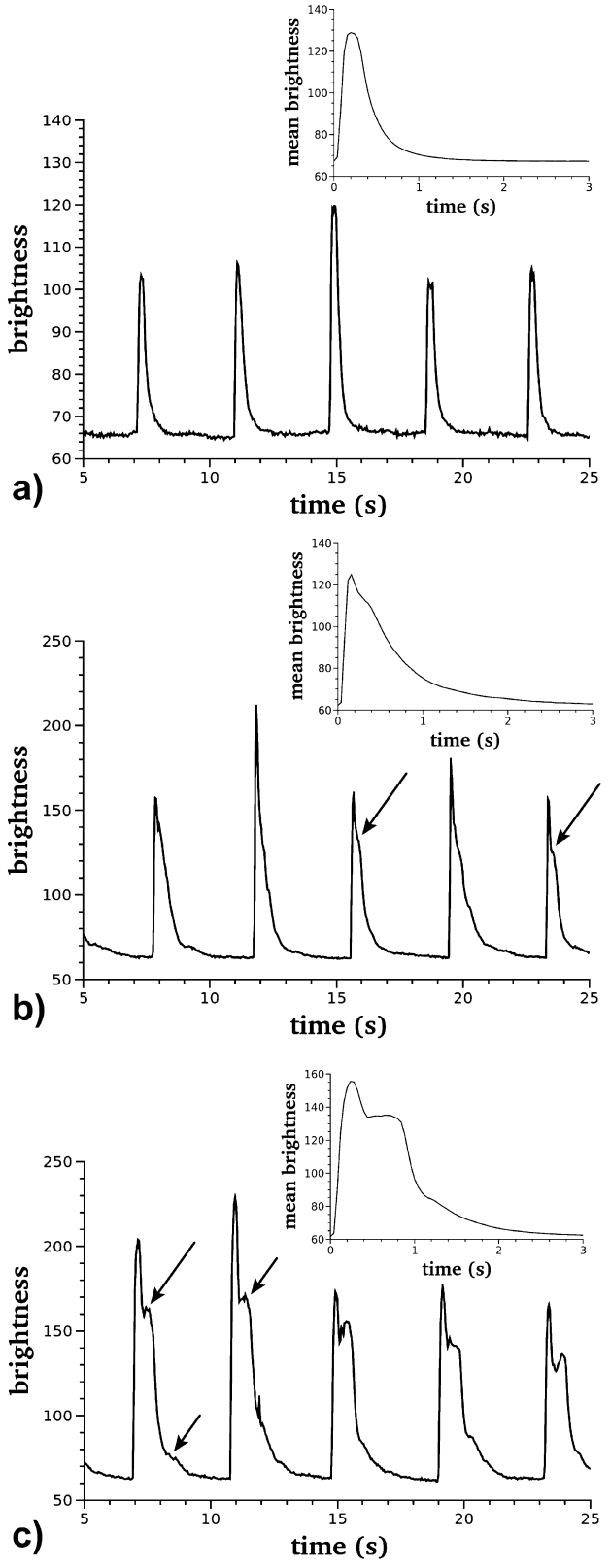

Figure 2. Experimental time series and their periodic average (insets) during (a) monomodal periodic oscillations (reaction conditions: T = 390 K, $F_{tip} \approx 4$ V/nm, $P_{H_2}/P_{NO_2} = 7.2$, $P_{NO_2} = 5.0 \times 10^{-4}$ Pa, $P_{H_2} = 3.6 \times 10^{-3}$ Pa); (b) coexistence of mono- and bimodal oscillations (T = 390 K, $F_{tip} \approx 4$ V/nm, $P_{H_2}/P_{NO_2} = 9.4$, $P_{NO_2} = 5.4 \times 10^{-4}$ Pa, $P_{H_2} = 5.1 \times 10^{-3}$ Pa); (c) bimodal periodic oscillations (T = 390 K, $F_{tip} \approx 4$ V/nm, $P_{H_2}/P_{NO_2} = 20.3$, $P_{NO_2} = 3.9 \times 10^{-4}$ Pa, $P_{H_2} = 7.9 \times 10^{-3}$ Pa).

dx.doi.org/10.1021/jp412506e | J. Phys. Chem. C 2014, 118, 6839−6846

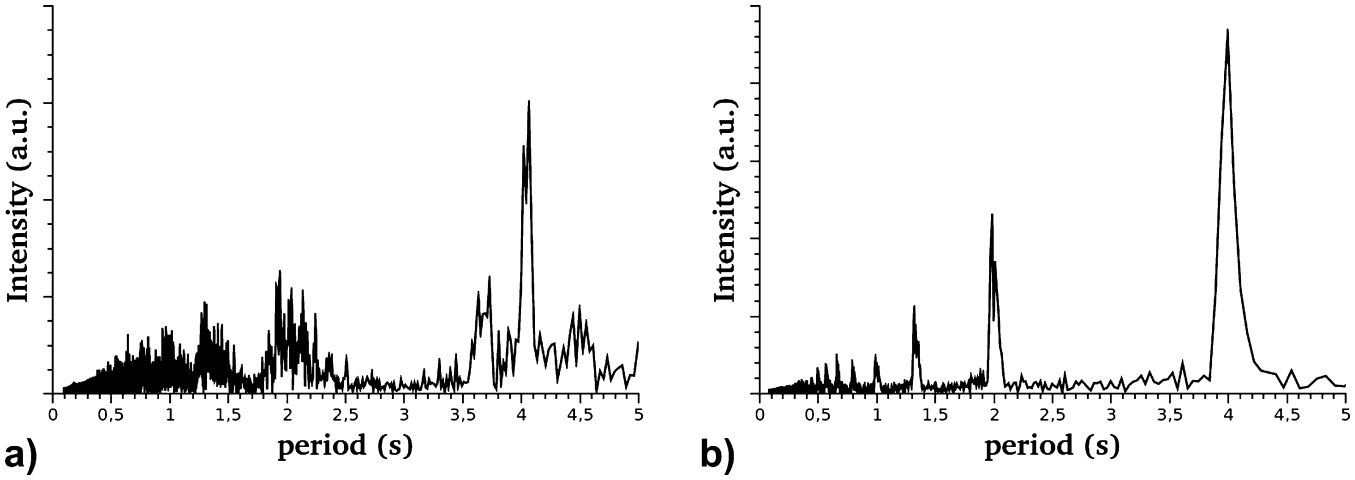

Figure 3. Power spectrum of the experimental time series (a) for the monomodal case (presented in Figure 2a), which shows a monotonous decrease in the amplitude of the harmonics; (b) for the bimodal case (presented in Figure 2c) showing a decrease in the amplitude, followed by a small increase at around 0.65 s.

that all the active regions (i.e., all the {012} facets) ignite simultaneously within 40 ms, which is the temporal resolution of the video recorder used for this study.

From the viewpoint of nonlinear dynamics, the observed oscillations are consistent with the existence of an underlying "noisy" limit cycle. The periodic character of the observed dynamics can be confirmed by Fourier power spectra of the time series or of its autocorrelation function, which show a well-defined period, for example, ~3.94 s for the time series of Figure 3a. The autocorrelation function itself displays damped oscillations.[48] This damping reflects a decrease of the correlation between oscillations separated by long intervals. This decrease is the consequence of compositional fluctuations, which affect the duration of oscillations since they make trajectories diffuse along the underlying limit cycle in phase space.[49−51]. It should be noted that large fluctuations of amplitude can be observed quite frequently. The resulting rather large dispersion of amplitudes suggests that fluctuations transversal to this underlying limit cycle are important in our case. Note that very similar features, that is, robust periods together with highly fluctuating amplitudes, were observed for models of chemical oscillators with a strongly nonlinear feedback.[52]

It is remarkable that the period of oscillation is so regular despite the presence of strong fluctuations of the surface composition between the pulses. This robustness can be quantified by the half-time of the envelope of the autocorrelation function, which is usually seen to extend over several periods. The reactive system under consideration, despite its very small size, thus, behaves as a *chemical nanoclock*. Such behavior has already been observed in a FIM study of the $O_2 + H_2$ reaction on Rh tips for which a detailed mechanistic model has been devised.[53] In this context, the $NO_2 + H_2$ system is characterized by an unprecedented regularity.[54] The reasons underlying such robustness at that scale are not fully understood thus far. The focus of our work therefore is to identify the complex oscillatory patterns and to provide clues for the reaction mechanism.

3.2. From Simple to Bimodal Oscillations. A gradual increase in the complexity of the oscillations could be observed when increasing the P_{H_2}/P_{NO_2} ratio. This trend is exemplified in Figure 2b,c, corresponding to P_{H_2}/P_{NO_2} = 9.4 and 20.3, respectively. In Figure 2b, one can observe that the sudden brightness peak is now *sometimes* followed by a shallow hump, which for larger pressure ratios (Figure 2c) turns into a fully developed secondary peak (see arrows in Figure 2b and 2c). The time between the two peaks was found to be relatively constant (about 0.5 s) and much larger than the time resolution of the detection system. In some instances, a third peak located approximately 0.5 s after the secondary peak could also be observed. Since the period of oscillations is of the order of a few seconds (4.0 s in Figure 2c), a dynamical phenomenon involving at least two distinct time scales is in operation. Note that the autocorrelation function of the signals has a damping half-time of about 30 s: the oscillations can thus still be regarded as robust.

Several analyses were performed in order to identify the class of complex oscillatory phenomena to which these observations belong. The power spectrum of the signal presents in each case a sharp and well-defined peak located at the main period. Secondary peaks (harmonics) can also be observed for fractions of this main period. The amplitude of these peaks decreases monotonously in the case of simple oscillations such as those reported in Figure 3a. When analyzing the above-mentioned complex oscillations (Figure 2c), though, the amplitude increases again when reaching 0.5 s. These features, and the very shape of the time series itself, are indicative of *bimodal oscillations*, in the sense that one has a superposition of modes characterized by a well-defined separation of time scales and amplitude. The Fourier power spectra being perturbed by considerable fluctuations, we turned to other data analysis methods to support this scenario.

Instead of treating the whole time series, as is done in a Fourier analysis or in classical phase space reconstruction, it is sometimes convenient to focus on *interevent intervals*. The basic idea behind such an approach is to first define a condition for the observable, and then to record the successive times at which this condition is fulfilled. This procedure generates a series of times, the properties of which can be analyzed to reveal regularities in the signal that would be difficult to highlight when considering all the details of the dynamics. These methods are very common in biology (neuroscience, cardiology, ...) and in earth science (earthquakes, climatic cycles, ...).[55,56]

dx.doi.org/10.1021/jp412506e | J. Phys. Chem. C 2014, 118, 6839−6846

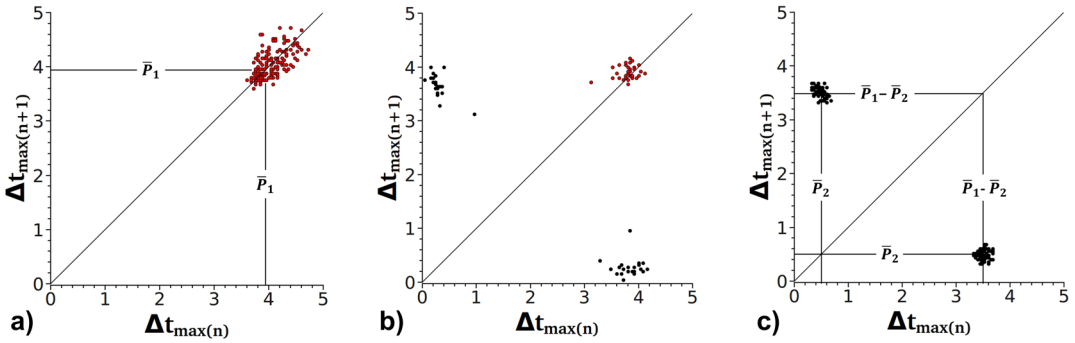

Figure 4. Interpeak interval maps reconstructed from the time series: (a) Map of the monomodal periodic oscillations (Figure 2a) showing a cloud of points centered on the average period of oscillations ($\overline{P}_1$, $\overline{P}_1$); (b) Map corresponding to the transition regime (Figure 2b); (c) Map of the bimodal periodic oscillations (Figure 2c), showing two distinct regions of points centered on ($\overline{P}_1-\overline{P}_2$, $\overline{P}_2$) and ($\overline{P}_2$, $\overline{P}_1-\overline{P}_2$), with $\overline{P}_2$ being the average time separation between the primary and the secondary peaks.

Interpeak intervals, that is, the times separating two successive maxima, form an especially useful quantity in the case of experimental results consisting of well-defined spikes (as the sharp oscillations observed here). One usually plots the time interval between two peaks as a function of the time interval separating the two previous peaks. Simple regular oscillations generate a single point in such maps, which is located at the time corresponding to the period. The interpeak interval maps constructed from the time series of Figure 2a–c are depicted in Figure 4. As expected, the simple regular oscillations observed in Figure 2a generate a cloud of points centered around the ($\overline{P}_1$, $\overline{P}_1$) position, $\overline{P}_1$ being the average period of oscillation (see Figure 4a). The dispersion of points around this value is indicative of the fact that fluctuations induce deviations of the interpeak intervals from the average period. Note, however, that these deviations are relatively small, which is consistent with the above-mentioned robustness of the oscillations' period.

In the case of Figure 2c, the corresponding map (Figure 4c) presents two distinct regions of points clustered around ($\overline{P}_1-\overline{P}_2$, $\overline{P}_2$) and ($\overline{P}_2$, $\overline{P}_1-\overline{P}_2$), $\overline{P}_2$ being the average time separating the principal and the secondary peaks. Such splitting reflects a qualitative change in the dynamics. The system comes back to a previously encountered interval only after going through an interval of a distinctly different length, that is, one now finds recurrence only every two peaks. The presence of two symmetric clouds of points thus forms a robust evidence of bimodal oscillations, which confirms the previous conclusions based on observing the original time series and the Fourier power spectra.

The case of oscillations such as those found in Figure 2b is especially interesting in that respect. As can be seen in Figure 4b, the interpeak interval map is then characterized by the coexistence of points clustered around ($\overline{P}_1$, $\overline{P}_1$) together with two other clusters located around ($\overline{P}_1-\overline{P}_2$, $\overline{P}_2$) and ($\overline{P}_2$, $\overline{P}_1-\overline{P}_2$). In this case, there is thus a coexistence of monomodal and bimodal oscillations. This can be further confirmed by visual inspection of the time series itself, in which it is found that sometimes double-peaked oscillations appear, even though they are not sustained. This effect is induced exclusively by the presence of noise in the system's dynamics. The state of the system continuously switches from monomodal to bimodal oscillations (and vice versa) because of spontaneous fluctuations of composition and fluctuations of the parameters.

Additional experiments were carried out to detect further transitions in the system, such as the emergence of n-modal ($n > 2$) oscillations. While some signs of increased modality could be observed in some instances, further analyses were impeded by strong background noise. In the conditions for which more complex oscillatory patterns could be observed, the amplitude of the fluctuations becomes comparable to the amplitude of the peaks. As a consequence, the different maps are more dispersed and it becomes increasingly difficult to define localized clouds of points.

Our focus in the remainder of this work will thus rather be on the physicochemical mechanism by way of which monomodal and bimodal oscillations could emerge in the system under consideration.

4. REACTION MECHANISM

How can the above dynamical picture be explained in terms of the chemical reactions taking place on the surface of the Pt tip? Answering this question requires a connection be made between the observed signal and the chemical composition of the surface. In FEM, the instantaneous state of the system is probed through a single observable: the local brightness of the emission pattern. The brightness depends on the work function of the probed facet, which is itself affected by the presence of adsorbates. It is thus useful to establish a list of likely species occurring during the reaction and to discuss their influence on the work function.

The NO_2 hydrogenation process on Pt has already been discussed in previous works.[53,57−59] It appears that NO_2(g) and H_2(g) both adsorb in a dissociative way on most Pt faces, leading to the formation of, respectively, NO(ads), O(ads), and H(ads). The initial (dissociative) sticking probability of NO_2 is higher though. NO(ads) can undergo further decomposition depending on the structure of the Pt microfacets[60] or simply desorb thermally[57,58] at the chosen reaction temperature. O(ads), N(ads), and H(ads) may combine to form intermediates such as OH and NH_x. Final products such as H_2, H_2O, and N_2 are expected to readily desorb at the working temperature. It is therefore anticipated that these molecules, after their formation on the surface, do not significantly influence the local brightness. Neither NH_3 nor N_2O are expected to form under our experimental conditions.

On the other hand, the mean residence time of O(ads) is much longer, as its desorption temperature is typically between 670 and 1300 K on Pt according to temperature programmed desorption studies.[57,58,61] The presence of important amounts of oxygen adatoms is therefore the most relevant information for the interpretation of the brightness pattern: since O(ads)

dx.doi.org/10.1021/jp412506e | J. Phys. Chem. C 2014, 118, 6839−6846

increases the work function, the image brightness is low under conditions of high O(ads) coverage. The fast increase in the brightness signal during the experiments must thus be associated with a fast decrease of the (local) O(ads) coverage due to water formation and desorption. This feature is common to both monomodal and bimodal oscillations. On the basis of this qualitative picture, at least two scenarios of the fast oxygen-to-water clean-off reaction can be considered:

Mechanism 1. In view of the available literature, it appears that the most probable candidate for such a clean-off process is the rapid formation of water through the following succession of steps:

$$H(ads) + O(ads) \rightleftarrows OH(ads) + * \quad (1)$$

$$H(ads) + OH(ads) \rightarrow H_2O(ads) + * \quad (2)$$

$$H_2O(ads) \rightarrow H_2O(g) + * \quad (3)$$

$$2H(ads) + O(ads) \rightarrow H_2O(g) + 3* \quad (4)$$

where * denotes an empty surface site. It has been shown that the addition of the first hydrogen adatom to the oxygen adatom is the rate-limiting step for this reaction path.[62,63]

A second mechanism, frequently invoked in the literature,[63,64] reads as follows:

Mechanism 2.

$$2H(ads) + 2O(ads) \rightleftarrows 2OH(ads) + * \quad (5)$$

$$OH(ads) + OH(ads) \rightleftarrows H_2O(ads) + O(ads) \quad (6)$$

$$H_2O(ads) \rightarrow H_2O(g) + * \quad (7)$$

$$2H(ads) + O(ads) \rightarrow H_2O(g) + 3* \quad (8)$$

The occurrence of the reaction step 6 was demonstrated in scanning tunneling microscopy (STM) experiments using hydrogen to titrate preadsorbed oxygen on Pt (111) at low temperatures.[65] Under such conditions, O(ads) and H_2O(ads) can coexist before the reaction is completed by thermal desorption of water,[62,66] so OH(ads) forms spontaneously. At the relatively high temperature of our experiments, the fast desorption of water makes the occurrence of large amounts of OH(ads) rather unlikely.

Both mechanisms lead to a net release of three vacant sites per reaction cycle. A decision on which mechanism applies cannot be made solely on the basis of a brightness analysis of FEM patterns. In any case, a single fast and nonlinear reaction does not suffice to explain the emergence of oscillations.[67] To produce an oscillatory behavior, a suitable feedback mechanism has to be provided. With the experimental information available at present, this question cannot be answered satisfactorily. We therefore limit the discussion to a scenario which presently seems to best fit the existing experimental information.

Because of the high sticking probability of NO_2 on the clean Pt surface, the initial stages of adsorption are expected to lead to large O(ads) coverages. It is well-known that oxygen can migrate under the surface of Pt facets.[68] Because of the open structure of the (012) plane, O(ads) may substantially penetrate the surface so as to occupy such subsurface sites. An example is given in the case of rhodium in ref 69. This could give rise to a feedback mechanism leading to oscillations under the hypothesis that the dissociative sticking probability of NO_2 decreases because of this subsurface oxygen diffusion. This is a quite reasonable assumption, and such effects have been observed before for similar cases.[70] Moreover, oxygen subsurface diffusion inevitably leads to a geometrical surface reconstruction. Indeed, STM observations demonstrated a periodic hill-and-valley structure of the (012) plane after extended oxygen exposure.[71] The sticking probability of oxygen-containing molecules on such a surface oxide seemed to be drastically reduced. An example of this behavior can be found in ref 72.

Within this scenario, the relative probability of dissociative hydrogen adsorption increases upon oxygen diffusion below the surface, and the H(ads) coverage may eventually reach a critical value allowing for substantial reaction with O(ads). For monomodal oscillations, observed at relatively low H_2 partial pressures, mainly O(ads) and little O(sub) would be titrated to form H_2O under these conditions. Upon increasing the H_2 partial pressure, bimodal oscillations would arise due to the more efficient removal of O(sub).

While the above feedback mechanism appears plausible in view of the existing literature, we do not exclude alternative scenarios to apply. For example, site blocking effects by species with sufficient surface lifetime or a redistribution of adsorption sites due to surface reconstruction might provide the necessary feedback to produce oscillatory behavior in a Langmuir–Hinshelwood type mechanism.[73] A deepening of these considerations must await further experiments, however. For example, we plan to perform field pulse experiments so as to receive information about the mean lifetime of NO(ads) species in the presence of O(ads). Furthermore, FIM will be employed to investigate the oxygen-induced reconstruction of the {012} facets after NO_2 adsorption and dissociation on a Pt tip.

5. CONCLUSION AND OUTLOOK

We have studied the catalytic hydrogenation of NO_2 on platinum nanocrystals by means of real-time field emission microscopy. The reactive system has been kept far from equilibrium via a constant supply of reactants in a continuously pumped reactor. Several nonlinear behaviors have been observed: self-sustained periodic oscillations of high regularity, as well as bimodal periodic oscillations characterized by the presence of a double peak in the brightness signal.

The different regimes have been identified via power spectra as well as interpeak analyses. Monomodal oscillations have been observed at low H_2/NO_2 pressure ratios, while bimodal oscillations could be correlated with larger hydrogen pressures. The transition between these two regimes has been shown to correspond to a fluctuation-induced coexistence of monomodality and bimodality, with some cycles presenting only a small hump after the peak of oscillation. These results point to the important role played by fluctuations of composition in the transition between the different regimes.

Two mechanisms of oscillatory water formation have been proposed, which qualitatively explain the occurrence of oscillations. Suggestions for the reasons behind the appearance of the bimodal oscillations have been made, including the existence of a reversible oxygen subsurface species. It is important to note that these scenarios represent only plausible explanations for the observed behaviors, based on the available knowledge and literature. We do not exclude that other phenomena could be present and play an important role on the

dx.doi.org/10.1021/jp412506e | J. Phys. Chem. C 2014, 118, 6839–6846

dynamics. Further experiments and concurrent modeling will be required in order to discriminate between the different possibilities. Another important aspect that should be addressed in the future is whether the system can undergo transitions to higher complexity. It is indeed well-known that such cascading transitions can lead to chaos, a behavior that has never been observed so far at such a small scale.

AUTHOR INFORMATION

Corresponding Authors

*E-mail: tvisart@ulb.ac.be. Tel.: +32 2 650 5724.
*E-mail: nkruse@ulb.ac.be. Tel.: +32 2 650 5714.

Notes

The authors declare no competing financial interest.

ACKNOWLEDGMENTS

C.B. thanks the Fonds de la Recherche Scientifique (F.R.S.-FNRS) for financial support (PhD grant). The authors gratefully thank the Van-Buuren Foundation for a financial support for the acquisition of equipment and the Wallonia-Brussels Federation (Action de Recherches Concertées No. AUWB 2010-2015/ULB15). The authors also thank Prof. Pierre Gaspard for fruitful discussions regarding the data processing of the nonlinear kinetics behaviors reported in this article.

REFERENCES

(1) Müller, E. W.; Tsong, T. T. *Field Ion Microscopy, Principles and Applications*; Elsevier: Amsterdam, 1969.
(2) Müller, E. W.; Tsong, T. T. Field Ion Microscopy, Field Ionization and Field Evaporation. *Prog. Surf. Sci.* **1974**, *4*, 1−139.
(3) Antczak, G.; Ehrlich, G. Jump Processes in Surface Diffusion. *Surf. Sci. Rep.* **2007**, *62*, 39−61.
(4) Kellogg, G. L. Field Ion Microscope Investigations of Adatom and Dimer Diffusion Along Rh(100) Step Edges. *Surf. Sci.* **1996**, *37*, 237−244.
(5) Gomer, R. Applications of Field Emission to Chemisorption. *Surf. Sci.* **1978**, *70*, 19−31.
(6) Condon, G. R.; Panitz, J. A. Mapping the Field-Emission Tunneling Barrier of Organic Adsorbates on Tungsten. *J. Vac. Sci. Technol. B* **2000**, *18*, 1216−1221.
(7) Medvedev, V. K.; Suchorski, Yu.; Block, J. H. Investigation of Adsorption and Coadsorption of O_2 and CO on Rh by O_2^+ Field Ion and Li^+ Field Desorption Microscopies. *Appl. Surf. Sci.* **1995**, *87−88*, 159−165.
(8) Bagot, P. A. J.; Cerezo, A.; Smith, G. D. W. 3D Atom Probe Study of Gas Adsorption and Reaction on Alloy Catalyst Surfaces II: Results on Pt and Pt-Rh. *Surf. Sci.* **2007**, *601*, 2245−2255.
(9) Visart de Bocarmé, T.; Moors, M.; Kruse, N.; Atanasov, I. S.; Hou, M.; Cerezo, A.; Smith, G. D. W. Surface Segregation of Au-Pd Alloys in UHV and Reactive Environments: Quantification by a Catalytic Atom Probe. *Ultramicroscopy* **2009**, *109*, 619−624.
(10) Visart de Bocarmé, T.; Bär, T.; Kruse, N. Field Ion Microscopy Study of the Structural Changes in Rh Crystals During the Reaction of Oxygen-Hydrogen Gas Mixtures. *Surf. Sci.* **2000**, *454−456*, 320−325.
(11) Gaussmann, A.; Kruse, N. Field Ion Microscopy of the CO-Induced Structural Changes of Pd and Pt Single Crystal Planes. *Surf. Sci.* **1992**, *266*, 46−50.
(12) Moors, M.; Visart de Bocarmé, T.; Kruse, N. Surface Reaction Kinetics Studied With Nanoscale Lateral Resolution. *Catal. Today* **2007**, *124*, 61−70.
(13) Gorodetskii, V. V.; Drachsel, W. Kinetic Oscillations and Surface Waves in Catalytic CO + O_2 Reaction on Pt Surface Field Electron Microscope, Field Ion Microscope and High Resolution Electron Energy Loss Studies. *Appl. Catal., A* **1999**, *188*, 267−275.
(14) Cobden, P. D.; de Wolf, C. A.; Smirnov, M.Yu.; Makeev, A.; Nieuwenhuys, B. E. Non-Linear Processes on Pt, Rh, Pd, Ir and Ru Surfaces During the NO-Hydrogen Reactions. *J. Mol. Catal. A: Chem.* **2000**, *158*, 115−128.
(15) Gorodetskii, V. V.; Elokhin, V. I.; Bakker, J. W.; Nieuwenhuys, B. E. Field Electron and Field Ion Microscopy Studies of Chemical Wave Propagation in Oscillatory Reactions on Platinum Group Metals. *Catal. Today* **2005**, *105*, 183−205.
(16) Visart de Bocarmé, T.; Bär, T.; Kruse, N. In Situ Dynamic Study of Hydrogen Oxidation on Rhodium. *Ultramicroscopy* **2001**, *89*, 75−82.
(17) Theiss, A.; Röllgen, F. W. Negative Field Ion Microscopy of the Initial Stages of Polymerization of Tetracyanoethylene. *Appl. Surf. Sci.* **1994**, *76/77*, 307−311.
(18) Sieben, B.; Bozdech, G.; Ernst, N.; Block, J. H. On the Kinetics of Oscillating Reactions: H_2/O_2 and H_2/H_2O on Platinum. *Surf. Sci.* **1996**, *352−354*, 167−172.
(19) Gorodetskii, V.; Lauterbach, J.; Rotermund, H.-H.; Block, J. H.; Ertl, G. Coupling Between Adjacent Crystal Planes in Heterogeneous Catalysis by Propagating Reaction−Diffusion Waves. *Nature* **1994**, *370*, 276−279.
(20) Joo, S. H.; Park, J. Y.; Renzas, J. R.; Butcher, D. R.; Huang, W.; Somorjai, G. A. Size Effect of Ruthenium Nanoparticles in Catalytic Carbon Monoxide Oxidation. *Nano Lett.* **2010**, *10*, 2709−2713.
(21) Somorjai, G. A.; Park, J. Y. Evolution of the Surface Science of Catalysis From Single Crystals to Metal Nanoparticles Under Pressure. *J. Chem. Phys.* **2008**, *128*, 182504.1−182504.9.
(22) Imbihl, R. Nonlinear Dynamics on Catalytic Surfaces. *Catal. Today* **2005**, *105*, 206−222.
(23) Ertl, G.; Rotermund, H.-H. Spatiotemporal Pattern Formation in Reactions at Surfaces. *Curr. Opin. Solid State Mater. Sci.* **1996**, *1*, 617−621.
(24) Ertl, G. Self-Organization in Reactions at Surfaces. *Surf. Sci.* **1993**, *287/288*, 1−11.
(25) McEwen, J.-S.; Garcia Cantu Rosa, A.; Gaspard, P.; Visart de Bocarmé, T.; Kruse, N. Non-Equilibrium Surface Pattern Formation During Catalytic Reactions With Nanoscale Resolution: Investigations of the Electric Field Influence. *Catal. Today* **2010**, *154*, 75−84.
(26) Alhumaizi, K.; Aris, R. Chaos in a Simple Two-Phase Reactor. *Chaos, Solitons Fractals* **1994**, *4*, 1985−2014.
(27) Swinney, H. L. Observations of Order and Chaos in Nonlinear Systems. *Physica D* **1983**, *7*, 3−15.
(28) Berry, H. Chaos in a Bienzymatic Cyclic Model With two Autocatalytic Loops. *Chaos, Solitons Fractals* **2003**, *18*, 1001−1014.
(29) Argoul, F.; Arneodo, A.; Richetti, P. Experimental Evidence for Homoclinic Chaos in the Belousov-Zhabotinskii Reaction. *Phys. Lett. A* **1987**, *120*, 269−275.
(30) Elnashaie, S. S. E. H.; Harraz, H. M.; Abashar, M. E. Homoclinical Chaos and the Period-Adding Route to Complex Non-Chaotic Attractors in Fluidized Bed Catalytic Reactors. *Chaos, Solitons Fractals* **2001**, *12*, 1761−1792.
(31) Eiswirth, M.; Ertl, G. Kinetic Oscillations in the Catalytic CO Oxidation on a Pt(110) Surface. *Surf. Sci.* **1986**, *177*, 90−100.
(32) Argoul, F.; Roux, J. C. Quasiperiodicity in Chemistry: An Experimental Path in the Neighbourhood of a Codimension-Two Bifurcation. *Phys. Lett. A* **1985**, *108*, 426−430.
(33) Simoyi, R. H.; Wolf, A.; Swinney, H. L. One-Dimensional Dynamics in a Multicomponent Chemical Reaction. *Phys. Rev. Lett.* **1982**, *49*, 245−248.
(34) Pomeau, Y.; Roux, J. C.; Rossi, A.; Bachelart, S.; Vidal, C. Intermittent Behavior in the Belousov-Zhabotinsky Reaction. *J. Phys. Lett.* **1981**, *42*, 271−273.
(35) Petrov, V.; Scott, S. K.; Showalter, K. Mixed-Mode Oscillations in Chemical Systems. *J. Chem. Phys.* **1992**, *97*, 6191−6198.
(36) Larter, R.; Steinmetz, C. G. Chaos Via Mixed-Mode Oscillations. *Philos. Trans. R. Soc., A* **1991**, *337*, 291−298.
(37) Lashina, E. A.; Slavinskaya, E. M.; Chumakova, N. A.; Stonkus, O. A.; Gulyaev, R. V.; Stadnichenko, A. I.; Chumakov, G. A.; Boronin,

A. I.; Demidenko, G. V. Self-Sustained Oscillations in CO Oxidation Reaction on PdO/Al_2O_3 Catalyst. *Chem. Eng. Sci.* **2012**, *83*, 149−158.
(38) Imbihl, R. Oscillatory Reactions on Single Crystal Surfaces. *Prog. Surf. Sci.* **1993**, *44*, 185−343.
(39) Eiswirth, M.; Krischer, K.; Ertl, G. Transition to Chaos in an Oscillating Surface Reaction. *Surf. Sci.* **1988**, *202*, 565−591.
(40) Razón, L. F.; Chang, S.-M.; Schmitz, R. A. Chaos During the Oxidation of Carbon Monoxide on Platinum − Experiments and Analysis. *Chem. Eng. Sci.* **1986**, *41*, 1561−1576.
(41) Van Tol, M. F. H.; de Maaijer-Gielbert, J.; Nieuwenhuys, B. E. Critical Size of Surfaces and Means of Synchronization for the Oscillating Reduction of NO by NH_3 Over Rh. *Chem. Phys. Lett.* **1993**, *205*, 207−2012.
(42) Ehsasi, M.; Scidel, C.; Ruppender, H.; Drachsel, W.; Block, J. H.; Christmann, K. Kinetic Oscillations in the Rate of CO Oxidation on Pd(110). *Surf. Sci.* **1989**, *210*, L198−L208.
(43) Suchorski, Yu.; Beben, J.; Imbhil, R.; James, E. W.; Liu, D.-J.; Evans, J. W. Fluctuations and Critical Phenomena in Catalytic CO Oxidation on Nanoscale Pt Facets. *Phys. Rev. B: Condens. Matter* **2001**, *63*, 165417.1−165417.12.
(44) Ladas, S.; Imbihl, R.; Ertl, G. Kinetic Oscillations during the Catalytic CO Oxidation on Pd(110): The Role of Subsurface Oxygen. *Surf. Sci.* **1989**, *219*, 88−106.
(45) Gaussmann, A.; Kruse, N. CO-Induced Structural Changes of Pd Particle Surfaces. *Catal. Lett.* **1991**, *10*, 305−315.
(46) Brown, D. *Tracker Video Analysis and Modeling Tool*, Version 4.80, 2009; http://www.cabrillo.edu/∼dbrown/tracker/.
(47) Anishchenko, V. S.; Astakhov, V.; Neiman, A.; Vadivasova, T.; Schimansky-Geier, L. *Nonlinear Dynamics of Chaotic and Stochastic Systems*; Springer: New York, 2007.
(48) McEwen, J.-S.; Gaspard, P.; De Decker, Y.; Barroo, C.; Visart de Bocarmé, T.; Kruse, N. Catalytic Reduction of NO_2 With Hydrogen on Pt Field Emitter Tips: Kinetic Instabilities on the Nanoscale. *Langmuir* **2010**, *26*, 16381−16391.
(49) Gaspard, P. The Correlation Time of Mesoscopic Chemical Clocks. *J. Chem. Phys.* **2002**, *117*, 8905−916.
(50) Baras, F.; Malek Mansour, M.; Van den Broeck, C. Asymptotic Properties of Coupled Nonlinear Langevin Equations in the Limit of Weak Noise. II: Transition to a Limit Cycle. *J. Stat. Phys.* **1982**, *28*, 577−587.
(51) Tomita, K.; Ohta, T.; Tomita, H. Irreversible Circulation and Orbital Revolution Hard Mode Instability in Far-from-Equilibrium Situation. *Prog. Theor. Phys.* **1974**, *52*, 1744−1765.
(52) Gonze, D.; Halloy, J.; Gaspard, P. Biochemical Clocks and Molecular Noise: Theoretical Study of Robustness Factors. *J. Chem. Phys.* **2002**, *116*, 10997−11010.
(53) McEwen, J.-S.; Gaspard, P.; Visart de Bocarmé, T.; Kruse, N. Nanometric Chemical Clocks. *Proc. Natl. Acad. Sci. U.S.A.* **2009**, *106*, 3006−3010.
(54) Barroo, C.; Visart de Bocarmé, T.; Kruse, N.; De Decker, Y. manuscript in preparation.
(55) Amiri, M.; Davoodi-Bojd, E.; Bahrami, F.; Raza, M. Bifurcation Analysis of the Poincaré Map Function of Intracranial EEG Signals in Temporal Lobe Epilepsy Patients. *Math. Comput. Simulat.* **2011**, *81*, 2471−2491.
(56) Hainzl, S.; Scherbaum, F.; Beauval, C. Estimating Background Activity Based on Interevent-Time Distribution. *Bull. Seismol. Soc. Am.* **2006**, *96*, 313−320.
(57) Bartram, M. E.; Windham, R. G.; Koel, B. E. The Molecular Adsorption of Nitrogen Dioxide on Pt(111) Studied by Temperature Programmed Desorption and Vibrational Spectroscopy. *Surf. Sci.* **1987**, *184*, 57−74.
(58) Huang, W.; Jiang, Z.; Jiao, J.; Tan, D.; Zhai, R.; Bao, X. Decomposition of NO_2 on Pt(110): Formation of a New Oxygen Adsorption State. *Surf. Sci.* **2002**, *506*, L287−L292.
(59) Voss, C.; Kruse, N. Oscillatory Behavior in the Catalytic Reduction of NO and NO_2 With Hydrogen on Pt Field Emitter Tips. *Appl. Surf. Sci.* **1996**, *94*−*95*, 186−193.
(60) Banholzer, W. F.; Park, Y. O.; Mak, K. M.; Masel, R. I. A Model for the Plane to Plane Variations in Catalytic Activity Seen During Nitric Oxide Decomposition on Platinum. *Surf. Sci.* **1983**, *128*, 176−190.
(61) Lu, K. E.; Rye, R. R. Flash Desorption and Equilibration of H_2 and D_2 on Single Crystal Surfaces of Platinum. *Surf. Sci.* **1974**, *45*, 677−695.
(62) Michaelides, A.; Hu, P. A Density Functional Theory Study of Hydroxyl and the Intermediate in the Water Formation Reaction on Pt. *J. Chem. Phys.* **2001**, *114*, 513−519.
(63) Michaelides, A.; Hu, P. Catalytic Water Formation on Platinum: A First-Principles Study. *J. Am. Chem. Soc.* **2001**, *123*, 4235−4242.
(64) Anton, A. B.; Cadogan, D. C. The Mechanism and Kinetics of Water Formation on Pt(111). *Surf. Sci.* **1990**, *239*, L548−L560.
(65) Völkening, S.; Bedürftig, K.; Jacobi, K.; Wintterlin, J.; Ertl, G. Dual-Path Mechanism for Catalytic Oxidation of Hydrogen on Platinum Surfaces. *Phys. Rev. Lett.* **1999**, *83*, 2672−2675.
(66) Karlberg, G. S.; Olsson, F. E.; Persson, M.; Wahnstrom, G. Energetics, Vibrational Spectrum, and Scanning Tunneling Microscopy Images for the Intermediate in Water Production Reaction on Pt(111) from Density Functional Calculations. *J. Chem. Phys.* **2003**, *119*, 4865−4872.
(67) Eiswirth, M.; Bürger, J.; Strasser, P.; Ertl, G. Oscillating Langmuir-Hinshelwood Mechanisms. *J. Phys. Chem.* **1996**, *100*, 19118−19123.
(68) Sadeghi, P.; Dunphy, K.; Punckt, C.; Rotermund, H. H. Inversion of Pattern Anisotropy During CO Oxidation on Pt(110) Correlated with Appearance of Subsurface Oxygen. *J. Phys. Chem. C* **2012**, *116*, 4686−4691.
(69) Rebholz, M.; Prins, R.; Kruse, N. Subsurface Oxygen and Its Influence on the Chemisorption Behavior of CO on Rh(210). *Surf. Sci.* **1992**, *269*−*270*, 293−299.
(70) Berdau, M.; Moldenhauer, S.; Hammoudeh, A.; Block, J. H.; Christmann, K. Interaction of Oxygen With Pt(210): Formation of New Oxygen States at Higher Exposures. *Surf. Sci.* **2000**, *446*, 323−333.
(71) Sander, M.; Imbihl, R.; Schuster, R.; Barth, J. V.; Ertl, G. Microfacetting of Pt(210) Induced by Oxygen Adsorption and by Catalytic CO Oxidation. *Surf. Sci.* **1992**, *271*, 159−169.
(72) Zhu, J. F.; Kinne, M.; Fuhrmann, T.; Tränkenschuh, B.; Denecke, R.; Steinrück, H.-P. The Adsorption of NO on an Oxygen Pre-Covered Pt(111) Surface: In Situ High-Resolution XPS Combined With Molecular Beam Studies. *Surf. Sci.* **2003**, *547*, 410−420.
(73) Battogtokh, D. Nonlinear Effects in the Site Blocking Induced Oscillations in the Catalytic Reaction of CO Oxidation. *Prog. Theor. Phys., Suppl.* **2006**, *161*, 165−168.